BONE ANISOTROPY INFLUENCE - A FINITE ELEMENT ANALYSIS

P. P. Kenedi*,**, L. L. Vignoli**,***

* PPEMM- Programa de Pós-Graduação em Engenharia Mecânica e Tecnologia dos Materiais - CEFET/RJ - Av. Maracanã, 229 - Maracanã - RJ - CEP 20271-110 - Brazil
** DEMEC - Departamento de Engenharia Mecânica - CEFET/RJ - Av. Maracanã, 229 - Maracanã - RJ - CEP 20271-110 – Brazil
*** Mechanical Eng. Dept., Catholic University of Rio de Janeiro, PUC-Rio, R. Marques de São Vicente 225, Gávea, Rio de Janeiro, RJ, Brazil, 22451-900

email: pkenedi@cefet-rj.br

Abstract: Bones are non-homogeneous, porous and anisotropic. Bone is a live tissue, it can grow, self-repair when damaged, and continuously being renewed by internal remodeling. It is accepted that the main path of bone remodeling process overlaps the principal stresses angles. Although this process makes it stronger, it makes bone quite anisotropic. A finite element analysis shows the influence of three constitutive options (isotropic, transversally isotropic and orthotropic) to, both, principal stress/strain and principal angles results.
Keywords: bone anisotropy, finite element, principal stresses

Introduction

The bone structure is responsible for sustaining the human body, and thus, is submitted to the action of the muscles loads. A femur, for instance, provides stability and support for a person to remain standing or walking.

In this work, a four forces model, adapted from [1], is used to generate the static loading condition at proximal femur of a Finite Element (F.E.) model. Three different constitutive models (orthotropic, transversally isotropic and isotropic) were used to estimate principal stress/strain values and principal angles, at medial external surface of a human femur, at a specific path, see [2]. In this work, the results shows that the principal angles at a medial external surface of a human femur have values compatible with [3] propositions, where the dominant osteonal direction is related with the first principal stress angle.

Material Anisotropy

Bone is, from macroscopic viewpoint, a non-homogeneous, porous and anisotropic tissue [4]. In a human femur can exist cortical and trabecular bone tissues. In this work a medial cross section was analyzed, where only cortical bone (mineralized and dense tissue) exists.

It is very difficult to obtain experimentally the bone elastic mechanical properties. Some authors like [5] have obtained orthotropic bone elastic properties indirectly, through the utilization of modal analysis and Finite Element Method approach.

[6] and [7] presents the differences between constitutive models. Among them, three are especially important for this work, the isotropic, the transversally isotropic and the orthotropic constitutive models. The isotropic materials have only two independent mechanical elastic constants, the Young modulus E and the Poisson ratio v. The transversally isotropic materials have five independent mechanical elastic constants, two Young moduli, one shear moduli and two Poisson ratio. The orthotropic materials have nine independent mechanical elastic constants, three Young moduli, three shear moduli and three Poisson ratios.

These mechanical elastic constants are placed at the stiffness matrix S, which relates stresses and strains. In a general way, the Hooke's law can be written as

$$e_{jr} = S_{jrlm}\tau_{lm} \tag{1}$$

where e is the strains, S is the stiffness, τ is the stresses and j,r,l,m = 1,2,3 (e, S and τ are matrices).

Finite Element Model

For this model, the loading is composed by the joint reaction force and three principal muscles forces, that are positioned at the femur head region, as shown at Figure 1, adapted from [1].

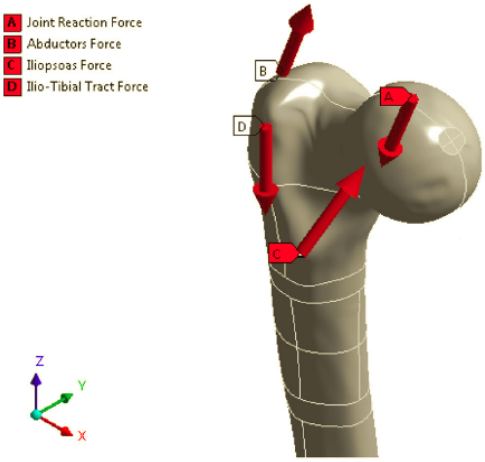

Figure 1: Femur schematic load.

The numerical model was developed with the F. E. ANSYS software. The bottom side of the bone is fixed to ensure equilibrium requirements. To extract the results, one path, on the medial cross section along the bone external surface, was created, as shown in Figure 2. The purple arrow indicates the path orientation.

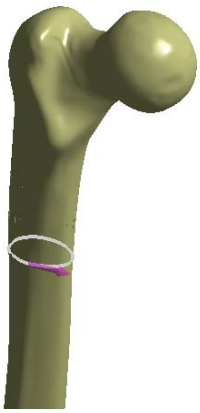

Figure 2: Path created to extract the results.

Figure 3 shows the mesh used at the human femur bone. The mesh at medial section, where the path is located, was refined to access more realistic results. As the geometry has a quite irregular shape, hexagonal elements, with eight nodes, were used.

Three simulations were done, maintaining the loading, boundary conditions, geometry and mesh. Only the elastic mechanical properties were changed for each three cases (isotropic, transversally isotropic and orthotropic).

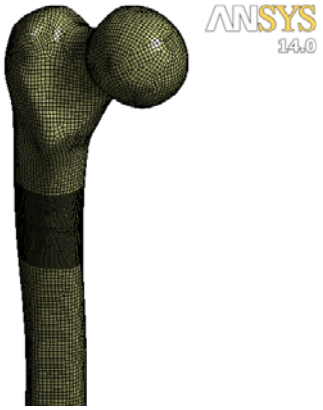

Figure 3: Mesh used on the F.E. simulations.

The range of these mechanical properties on the literature is wide. This can be explained by the existing differences between people's bones, as age, diseases, gender..., also the exact state of the bone specimen (fresh or frozen) influences the test results. Table 1 shows the used loading forces and geometric constants.

Table 1: Loading forces and geometric constants.

Joint reaction force - P_1 (N)	(–1,062; -130; -2,800)
Abductors force – P_2 (N)	(430; 0; 1,160)
Iliopsoas force – P_3 (N)	(78; 560; 525)
Iliotibial tract force – P_4 (N)	(0; 0; -1,200)
P_1 point of application (mm)	(50.7; -2.7; 158)
P_2 point of application (mm)	(-13.5; -6.5; 140)
P_3 point of application (mm)	(18.8; -29.3; 83.7)
P_4 point of application (mm)	(-24.6; -4.2; 108)
r_o (external radius) (mm)*	16
r_i (internal radius) (mm)*	7.66

* approximate measure

Table 2 shows the elastic mechanical properties obtained, in technical literature, for isotropic, transversally isotropic and orthotropic bone materials.

Table 2: Elastic mechanical properties.

Material Properties	**Isotropic [8]**	**Transversally Isotropic [9]**	**Orthotropic [10]**
E (GPa)	20	-	-
E_1 (GPa)	-	18.8	12
E_2 (GPa)	-	18.8	13.4
E_3 (GPa)	-	27.4	20
G (GPa)	8.1	-	-
G_{12} (GPa)	-	7.17	4.53
G_{23} (GPa)	-	8.71	6.23
G_{13} (GPa)	-	8.71	3.56
ν	0.3	-	-
ν_{12}	-	0.312	0.376
ν_{23}	-	0.193	0.234
ν_{13}	-	0.193	0.222

Results

In this section the results of the F.E. model, described on the previous section, are shown. The principal stresses and principal strains are presented, as well as, the respective principal angles, which are especially important to check if they can be related with bone lamellae orientation.

Figure 4 shows the maximum principal stresses distribution for orthotropic material.

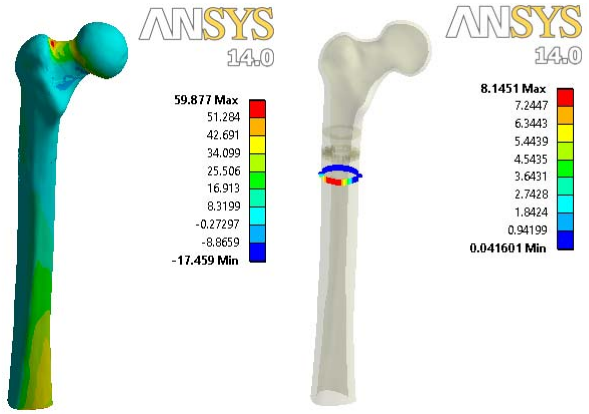

(a) (b)

Figure 4: Maximum principal stresses distribution for orthotropic material: (a) external surface and (b) path.

Note that using path approach, from 0º to 360º, makes possible a more precise results achievement.
For all next figures, Ortho, Trans and Iso are related, respectively, with orthotropic, transversally isotropic and isotropic materials. For Figures 5 and 6, the max, mid and min are related, respectively, to the maximum, middle and minimum principal stress/strain. The three principal stresses are plotted in Figure 5.

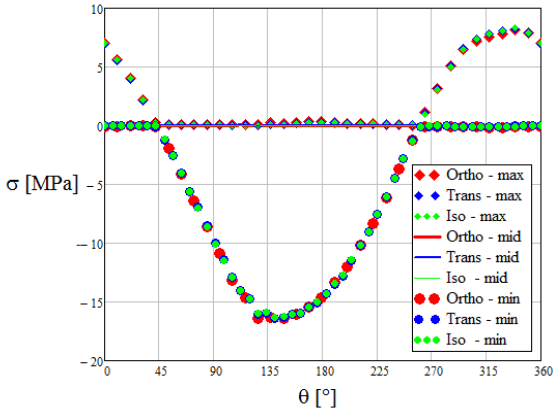

Figure 5: Principal stresses, at path.

Note that the path is along a free external surface, thus one of the principal stresses is always zero. The principal stresses modulus is almost equal for the three cases.

Figure 6 shows the principal strains results.

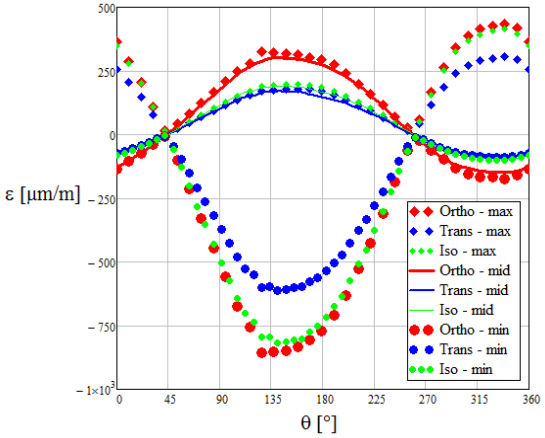

Figure 6: Principal strains, at path.

Note that although the principal strains distribution, maintained the main shape for three material cases, there are significant differences in strains values. Figures 7.a and 7.b show, respectively, the principal stress and strains angles.

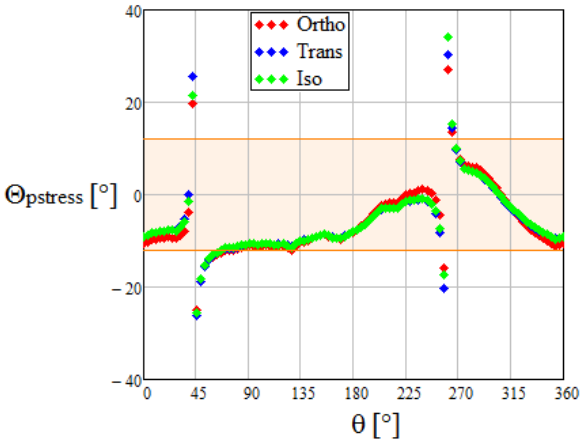

(a)

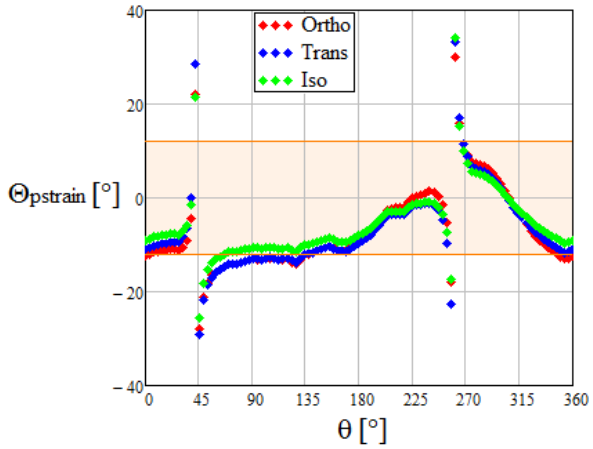

(b)

Figure 7: (a) Principal stresses angles and (b) principal strains angles, both, at path.

Figure 8 shows the difference between the principal strains and the principal stresses angles.

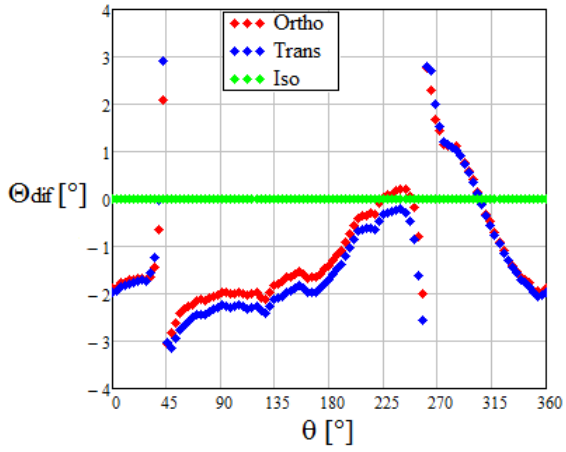

Figure 8: Difference between the principal strains and the principal stresses angles, at path.

Figure 8 shows that there are no differences between principal stresses and principal strains angles for isotropic case. For transversally isotropic and orthotropic cases, there are measurable differences.

Discussion

Three material cases (isotropic, transversally isotropic and orthotropic) were used to model the cortical bone tissue in a F.E. analysis. A path, at medial human femur cross section, was used to obtain the principal stress and the principal strains distribution as well the respective principal angles.

The range of principal stress angles values, shown at Figure 7.a, within the shaded area between -12º and +12º angles, were compatible with dominant osteonal range angles experimentally obtained by [2]. Also, for the three material cases, Figure 7.a shows little differences in principal stress angles and Figure 7.b shows substantial differences in principal strain angles.

Conclusion

The F.E. analysis shows that bone anisotropy was less important at principal stress distribution, but has a significant effect at principal strain distribution. Also, the principal stress angle distribution was less sensitive to bone anisotropy than the principal strain angle distribution.

In other words, the results show that it is important to take into account significant differences, mainly in principal strains values and principal strain angles, connected to the level of anisotropy of long bones cortical tissues.

Acknowledgements

The authors would like to acknowledge the support of CEFET/RJ PIBIC Program.

References

[1] Taylor, M.E., Tanner, K.E., Freeman, M.A.R. and Yettram, A.L., Stress and strain distribution within the intact femur: compression or bending?, Med. Eng. Phys., 1996, (18), No. 2, pp. 122-131.

[2] Petrtyl, M., Herf, J. and Fiala, P., Spatial Organization of the Haversian Bone in Man, J. Biomech., 1996, (29), No. 2, pp. 161-169.

[3] Cowin, S.C. and Hart, R.T., Errors in the orientation of the principal stress axes if bone tissue is modeled as isotropic, J. Biomech., Technical Note, 1990, (23), issue 4, pp. 349-352.

[4] Doblaré, M., García J. M. and Gómez, M. J., Modeling bone tissue fracture and healing: a review, Engineering Fracture Mechanics, 2004, (71), pp. 1809-1840.

[5] Taylor, W.R., Roland, E., Ploeg, H., Hertig, D., Klabunde, R., Warner, M.D., Hobato, M.C., Rakotomanana, L. and Clift, S.E., Determination of orthotropic bone elastic constants using FEA and modal analysis, J. Biomech., 2002, (35), pp. 767-773.

[6] Jones, R.M., Mechanics of Composite Materials, Second Edition, Taylor & Francis Editions, 1998.

[7] Krone, R. and Schuster, P., An Investigation on the Importance of Material Anisotropy in Finite-Element Modeling of the Human Femur, SAE International, 2006, 2006-01-0064.

[8] Kenedi, P.P., Riagusoff, I.I.T., Stress development at human femur by muscle forces, J Braz. Soc. Mech. Sci. Eng., 2014, Published online: 04 April 2014.

[9] Yoon, H.S., Katz, J.L., Ultrasonic wave propagation in human cortical bone—II. Measurements of elastic properties and microhardness.

[10] Korsa, R., Mares, T., Numerical Identification of Orthotropic Coefficients of the Lamella of a Bone's Osteon, Bulletin of Applied Mechanics, 2012, 8(31), pp. 45-53.